Stabilised control strategy for PEM fuel cell and supercapacitor propulsion system for a city bus

W. Wu, J.S. Partridge*, R.W.G. Bucknall

Dept. of Mechanical Engineering, UCL, UK

ARTICLE INFO

ABSTRACT

Fuel Cell (FC) buses have been developed as a long term zero emission solution for city transportation and have reached levels of maturity to supplement the coming London 2020 Ultra low emission zone implementation. This research developed a scaled laboratory Fuel Cell/Supercapacitor hybrid drivetrain implementing DC/DC converters to maintain the common busbar voltage and control the balance of power. A novel and simple hybrid control strategy based on balancing the currents on the common busbar whilst maintaining a stable FC output has been developed. It has been demonstrated that the FC power output can be controlled at a user defined value for both steady state and transient load conditions. The proposed control strategy holds the promise of extending FC life, downsizing power systems and improving the FC operating efficiency.

Introduction

Mechanised transportation is one of the largest sources of greenhouse gas emissions [1], where 30% of CO2 emissions from OECD countries is attributed to transport [2]. The harmful emissions from heavy traffic in a city not only contain greenhouse gases, contributing to climate change, but also particulate and NOx emissions that affect human physical health and well-being. In 2008 it was estimated that over 4000 premature deaths were brought forward as a result of long-term exposure to particulates in London [3]. The seriousness of city pollution resulting from the transportation sector has been acknowledged and thus the introduction of clean transport technologies that can effectively bring environmental benefits is of increasing priority.

One such technology is the Fuel Cell (FC), which is a clean and efficient power source that has undergone substantial development and is now a commercially viable means of offering a potentially clean solution. Various fuel cell technologies exist, where each technology has its own specific advantages, disadvantages and is for different applications. Proton Exchange Membrane Fuel Cells (PEMFC) have relatively high power densities and low weight; it can achieve high efficiency and operates at low temperature, and reflects why this is the most commonly used FC type for transportation applications [4]. The PEMFC uses hydrogen as its fuel and air as a reactant to generate electricity through an electrochemical process with water as the only waste product. The FC circumvents the combustion and mechanical processes, of a conventional internal combustion engine, into a single chemical step to generate electricity [5]. The PEMFC was not a practicable option for wider applications until the early 1990s owing to the need for significant amounts of rare and costly materials. Important advances in PEMFCs have been achieved, such as reducing the platinum catalyst loading from 25 mg/cm^2 to 0.05 mg/cm^2 [6]. This has resulted in the cost of the

---

Nomenclature

I_{fc_in}	Current output from the Fuel Cell
I_{fc_out}	Current output from the boost converter on the common busbar
I_{fc_ref}	Reference value for the boost converter current output on the common busbar
I_{load}	Current to/from the traction motor
I_{SC_in}	Current to/from the Supercapacitor
I_{SC_out}	Current to/from the Buck/Boost converter on the common busbar
V_{fc_in}	Voltage across the Fuel Cell
V_{fc_out}	Voltage across the Boost converter on the busbar
V_{load}	Voltage across the traction motor controller on the busbar
V_{SC_in}	Voltage across the supercapacitor
V_{SC_out}	Voltage across the Buck/Boost converter on the busbar

PEMFC dropping significantly since 2000, making the PEMFC a viable solution for transportation applications [7].

By replacing the internal combustion engine of conventional vehicles, FCs can be used to power the vehicle using electrical energy only, therefore achieving zero operating emissions since water is the only waste product. After initial assessments of FC vehicle technology and the introduction of hybrid technology in the early 2000s, researchers started to consider hybridising FCs with different energy storage technologies to provide more effective solutions [8–10]. A number of studies have suggested that the use of FCs is limited by an inability to react quickly to the power demand transients presented by transportation applications because of their low power density characteristics [11–13]. Hence, hybridisation of FC technology with electrical energy storage options has been utilised to shield the FC from transient peak power demands and effectively reduce the size of the FC required on-board the vehicle [13,14]. When compared with batteries, recent studies have proposed that Super-capacitors (SC) are a more effective energy storage technology for hybridisation with FCs in terms of responding to dynamic loads, shielding high current loads, reducing energy throughput and preventing overheating [15–17].

The development of hybrid propulsion systems can utilise the benefits of each of the system components to meet the load demands, however, the technologies used, topologies and energy management of such systems allows for a wide range of possible solutions. The literature contains many examples of FC based hybrid propulsion systems each with different aims and utilising different technologies. One approach to such a system was presented by Wu. et al. where the FC and SC were directly connected to give passive control of the hybrid system [11]. This approach provides an advantage in avoiding the need for DC/DC converters but at the cost of losing direct control of the power sharing of the system components and stability of the load voltage. The work presented in Refs. [18–21] considered FC/battery hybrid

propulsion systems, where a relatively small FC was used as a range extender and the battery as the main power source. This was able to significantly increase the range of the vehicle, however, the work presented in this paper is concerned with FC dominant hybrid systems, where the FC acts as the primary power source. Many possible configurations for FC based hybrid power systems exist. Much of the literature employs DC/DC converters in the hybrid system to provide direct control of some or all of the hybrid system components [17,21–33]. The work of Latha et al. presents the pros and cons of each of these system configurations and goes on to develop a novel reconfigurable hybrid propulsion system based on the use of DC/DC converters [22]. Another approach for a FC hybrid propulsion unit is to use a DC/DC converter to control the FC output, as seen in Refs. [25,30]. This has the advantage of using only one converter, however this comes at the expense of control of the DC-link voltage or power sharing control. The most popular configuration makes us of a uni-directional DC/DC converter for the FC and a bidirectional DC/DC converter for the SC, where these are connected via a common DC-link, as seen in Refs. [17,24,26–29,32,33]. This configuration is particularly useful when using a SC energy storage system as the voltage across the SC can be independent from the rest of the system. Since SCs have a wide voltage range over their State-of-Charge (SoC), it allows for better utilisation of the stored energy. Each of these systems utilise a different control strategy to split the power sharing between the FC and energy storage system but generally use the battery or SC to meet the short transient load changes to minimise the load variations on the FC. Even so each of these control strategies results in significant variations to the FC output. In the work of Torreglosa et al. the hybrid system was controlled with 8 different states of operation depending on the battery SoC, load demand and tramway speed [25]. The battery met much of the transient response with the FC operating at a number of different outputs. In the work of Bougrine et al. control strategies based on using the SoC as the state variable were developed to control the FC output [26]. The SC met the transient power demands thus damping the rate at which the FC output varied. Allaoua et al. presented a control strategy where all of the transient power demands are met by the SC and the FC is used only to meet the steady state power demands of the load [28]. This resulted in significant changes to the FC output when the load demands changed from transient to steady state. The system most closely resembling that developed in this paper was developed by Benyahia et al., where interleaved boost and bi-directional DC/DC converters were used with the FC boost converter was used to regulate the DC busbar voltage [24]. It was shown that the system was able to maintain a stable voltage on the busbar but as with all of the control strategies presented, the FC output was variable.

The work in this paper follows on from the research carried out in Ref. [13], where a laboratory FC system consisting of a FC, DC/DC boost converter and a resistor bank was constructed and tested. This paper extends the work through the integration of a SC module, traction motor and load system to form a FC/SC hybrid propulsion test bench. The configuration chosen makes use of two DC/DC converters, one unidirectional DC/DC converter for the FC and another

bidirectional DC/DC converter for the SC as is commonly used in the literature. A control strategy aimed at maintaining a constant FC output at a chosen value, thus eliminating the dynamic response of the FC, has been developed for the system and tested under both quasi-static and dynamic load conditions. This differs from the literature, where the FC output is generally variable. The proposed system is based on controlling the current in and out of the bidirectional DC/DC converter to balance the split of power in the system with the unidirectional DC/DC converter used to maintain the voltage on the common busbar. Balancing the current on the busbar also removes the requirement for knowledge of the efficiency of any of the DC/DC converters to provide power balancing. This provides a simple means of controlling the hybrid system, requiring a single user defined value to assign the output power of the unidirectional FC DC/DC converter. For this research it was decided that a scaled FC propulsion platform would be constructed, based on the propulsion system used in the FC/SC bus operating in London. This will allow for analysis of both the steady state performance of the system and the transient behaviour that characterises the operation of a city driving bus in real world operation, where regular stops and variable traffic conditions result in highly transient driving conditions. Hybridising the FC propulsion unit with the SC can reduce transient power demand on the FC, allowing for efficiency optimisation and output stabilisation of the FC. The SC, as the energy storage medium, can satisfy transient peak power demand and exploit regenerative braking energy recovery. This paper presents the development of a laboratory FC/SC hybrid propulsion system and a control strategy focusing on the power balancing between the FC, the SC and the load. The developed laboratory system was tested with a series of experiments to investigate the characteristics of FCs and SCs and how they interact in a hybrid propulsion system. Finally, the proposed control strategy was evaluated against a series of test as follows.

1. Quasi-steady state conditions to represent,
   a. Heavy bus loading.
   b. Light bus loading.
   c. Regenerative braking.
2. Dynamic conditions to represent,
   a. Simple dynamic cycle.
   b. Complex dynamic cycle.

Hybrid drivetrain operation mode

A FC/SC series hybrid propulsion structure has been proposed to represent the scaled bus power system. Three main modes of operation are expected to occur during bus driving operation and the power flow for each mode of operation is shown in Fig. 1.

- Mode 1: The SC will deliver energy to supplement the FC for high transient outputs. This type of operation is expected to occur during acceleration, climbing of gradients or under heavy loading.
- Mode 2: The FC will power the load and use excess power to charge the SC. This is expected to occur when the FC is providing more power than the load requirement.
- Mode 3: The power from the FC and power generated from regenerative braking will both be used to charge the SC. This is only expected to occur when the bus is in regenerative braking mode.

System configuration

To test the proposed FC/SC control strategy, a scaled FC/SC hybrid drive train has been developed as a laboratory test bench. The proposed hybrid drive train can be divided into three sub-systems: FC system, SC system and load system as shown in Fig. 2. The choice of system components has been chosen to loosely represent a downscaled model of the FC/SC hybrid bus in operation on the RV1 bus route in London, where an 75 kW PEM FC and a SC energy storage unit of 0.5 kWh is utilised. The specifications of the main components used in the system are outlined in Table 1. The system voltage for the common connection between the hybrid system components or busbar voltage was set at 48 Vdc. The installed laboratory test bench is shown in Fig. 3.

The FC system consists of a Hydrogenics HD8 8.5 kW PEM FC and an 8.5 kW boost converter manufactured by Custom Power Design. The FC stack power utilised for the RV1 bus is a 75 kW PEMFC from Ballard which gives a required power for the scaled FC unit to be 7.5 kW, thus the 8.5 kW PEMFC unit from Hydrogenics was selected as the closest option to
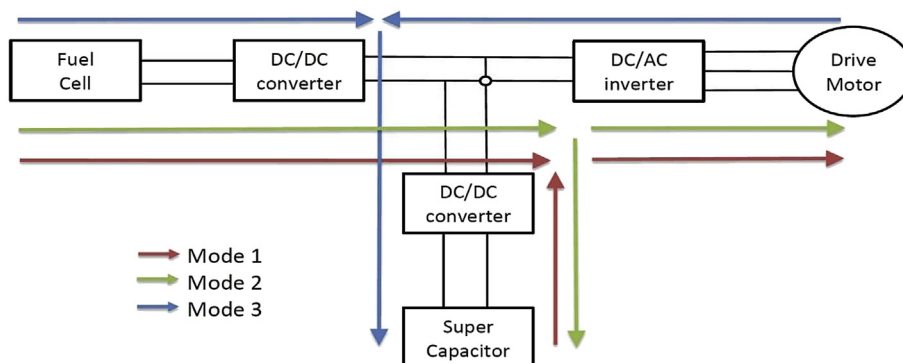

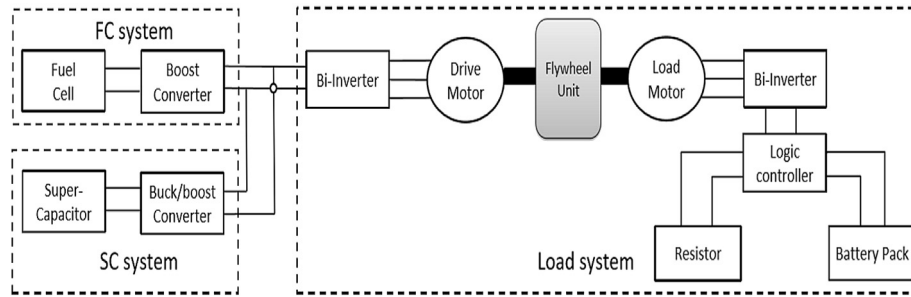**Fig. 1 — FC hybrid drivetrain operation modes and power flows.**

Fig. 2 — Structure of the laboratory FC/SC series hybrid system.

Table 1 — Summary of main components in the scaled FC/SC hybrid drivetrain.

FC system			
PEMFC		Boost converter	
Model	Hydrogenics HD8	Model	CPD SM5380
Rated power	8.5 kW	Rated power	8.5 kW
Operating current	0—380 A	Input voltage	20—40 V
Operating voltage	20—40 V	Output voltage	48 V
SC system			
SC		Buck/boost converter	
Model	Maxwell P048 B01	Model	AEP USCDCDC-6
Capacitance	83 F	Rated power	6 kW
Rated voltage	48 V	Operating voltage	0—80 V
Stored energy	0.027 kWh	Operating current	0—150 A
Load system			
Motor		**Inverter/motor controller**	
Model	HPEV AC-9	Model	Curtis 1234
Peak power	14.5 kW	Nominal voltage	36—48 V
Flywheel		**Logic controller**	
Model	Golconda	Model	Zelio SR3
Inertia of disc	0.705 kg.m^2	Output relay	24 V
Resistor bank		**Battery pack**	
Model	Pentagon type PT	Model	Halfords HB063
Resistance	1 Ω/unit	Voltage	4*12 V

Fig. 3 — a) Installed FC in the Lab b) Test rig for the SC system and load system in the lab.

Table 2 — Current-temperature correlation look up table for the FC.

Current (A)	Temperature (°C)
>125	65 (±2)
75—125	60 (±2)
55—75	55 (±2)
<55	50 (±2)

meet the 7.5 kW power requirement. A number of sub systems have also been specifically designed including the hydrogen supply system, ventilation system and cooling system. The hydrogen cylinders for the FC have been selected as standard size K at 175 bar pressure at 15 °C. The supply pressure for the FC has been regulated to provide a 1.2 bar stack operating pressure. The ventilation system consists of a set of pipeline connections and an exhaust blower to vent the anode and cathode exhausts with a dilution blower system. The cooling system consists of a set of pipeline connections and a coolant (deionised water) flow system. The cooling system has been designed to keep the FC inner temperature within the range of a current-temperature correlation look up table provided by the manufacturer as Table 2 shows.
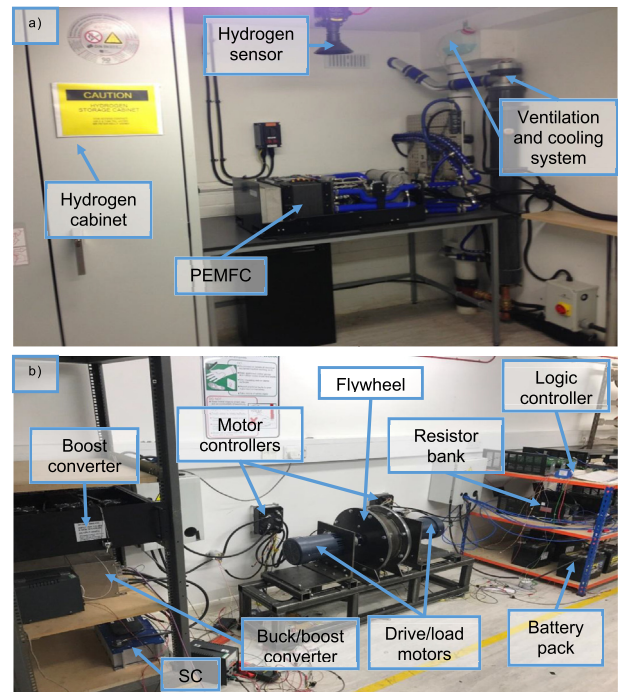
Since the FC output voltage will decrease when a higher output power has been demanded as a result of voltage losses in the FC, the boost converter for the FC has been designed to be a uni-directional DC/DC converter and acts to boost the FC output voltage to stable 48 V_{DC} on the common busbar.

The SC system consists of a SC and a buck/boost converter for the SC. The SC has been selected to have a rated voltage of 48 V. The Maxwell P048 B01 SC module has been selected from

Maxwell which is not only one of the largest SC manufacturers worldwide but also the SC supplier for the energy storage system on the London FC bus RV1. The SC is rated at 48 V and has a capacitance of 83 F.

A bi-directional buck/boost converter manufactured by AEP hybrid has been proposed to control the SC charge/discharge. Since the SC voltage is proportional to the SoC which means the SC voltage will vary as the SC is charging or discharging. Therefore, the converter to control the SC will not only control the power flow to the SC depending on the power demand, but also control the output voltage to the motor controller.

The load system consists of a motor/generator set, a flywheel and a motor loading system. The motor/generator set consists of two identical AC-9 AC induction machines manufactured by HPEVS. Each motor is controlled using a Curtis 1234 motor controller. The motor was selected such that the peak power was greater than the sum of the FC rated power and the Buck/Boost converter maximum output. The voltage of the common bus bar has been chosen to be 48 V for safety reasons. A flywheel, manufactured by Golconda, is connected between the two motors and acts to represent the inertial mass of the bus. The flywheel was sized to represent the mass of the bus, whereby a conversion factor was used to link the velocity of the bus to the motor shaft speed. The kinetic energy of the bus was determined for different speeds, with the energy contained within the flywheel at different shaft speeds being scaled to 10% of that of the bus. The motor on the FC side is the drive motor and acts as the traction motor of the bus, operating as part of the hybrid system. The motor on the other side is the load motor which is used to represent different load conditions on the FC/SC hybrid drivetrain. Under most conditions this acts as a generator where the electrical power generated is dissipated through a bank of power resistors. The resistance of the power bank is adjusted by turning on relays, depending on the power generated by the load machine, with these relays controlled through a logic controller. In addition, there is a battery bank used to keep the motor controller on when the motor is stationary and allows the load machine to be operated as a motor.

Control strategy

The proposed hybrid drivetrain represents the power system of a FC/SC series hybrid propulsion bus. A control strategy has been proposed based on the power density and energy density characteristics of the FC and the SC. Power density indicates how fast energy can be delivered or absorbed while energy density describes how much energy can be stored. The power and energy density characteristics of FCs and SCs have been presented in the Ragone plot shown in Fig. 4.

It can be seen from Fig. 4 that FCs have a high energy density but low power density while the SCs have a very high power density but low energy density. The high energy density of FCs makes them more suitable to work as a constant and steady power source while the high power density of SCs makes them suitable for any fast charge/discharge operations. The combination of these properties complement each other when working together in a hybrid system and was the reason
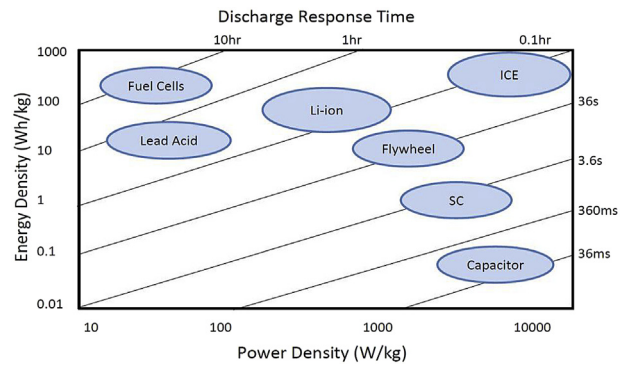

Fig. 4 – Ragone plot of main power sources and energy storage technologies. The plot has been produced using information from Luo et al. [34].

for choosing a FC/SC hybrid system. As a result, the control strategy has been proposed to keep the FC output near constant while using the SC to supplement any power demand that is higher than the FC output and recover energy captured through regenerative braking.

Unlike equivalent consumption minimisation strategies used in conventional electric hybrid vehicles, the developed control strategy has been designed to maintain a stable FC output power via controlling the current flow in the hybrid system. Fig. 5 shows the main components of the FC/SC system and descriptions of the voltage and current used in different parts of the system. It should be noted that there are a number of control systems present in the hybrid system. These are utilised in individual components to control the operation of the FC, traction motor, and power electronics. The control system detailed below is for the control of the balance of power in the hybrid system and is the focus of this paper.

The boost converter for the FC maintains a near constant 48 V potential (V_{fc_out}) at the bus bar of the hybrid system. This voltage also governs the voltage of V_{load} and V_{fc_out}. The buck/boost converter for the SC is used to control the output current (I_{sc_out}) to a user-defined value. The voltage potentials of V_{fc_out}, V_{sc_out} and V_{load} will be the same as they are all connected to a common bus bar. In effect this means that the flow of power between each of the components connected to the bus bar is governed only by the current flow at each of these components, with the relationship between the three currents formulated as:
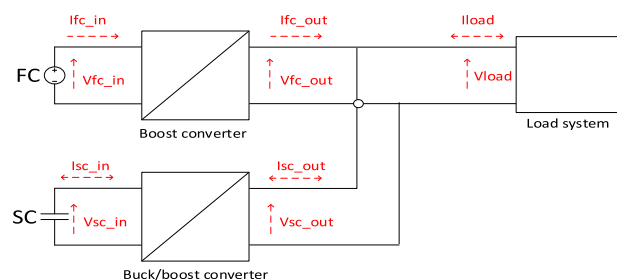

Fig. 5 – Main parameters in the FC/SC hybrid system.

$$Ifc_{out} + Isc_{out} = I_{load} \tag{1}$$

where Ifc_{out} is the output current from the boost converter, Isc_{out} is the output current from the buck/boost converter and I_{load} is current going in and out to the load. In this current relationship, the load current is defined by the power cycle, with the requirement that the FC and SC systems meet this demand at all times. The SC output current is defined by the user, whereas the FC output power will passively respond to provide the difference in current between I_{sc_out} and I_{load}. If a power cycle is applied on the FC hybrid control system, the FC would react to the load current demand minus the defined SC output current. However, this is counter to the design concept of the FC/SC hybrid system. The aim of this control algorithm is to control and keep the FC output as stable as possible to avoid numerous extreme transient power variations which could potentially damage the FC and reduce the overall FC efficiency. The FC/SC hybrid control system would have to be modified to meet this controlled FC constant current output requirement.

The proposed strategy is to assign a user defined reference value I_{fcref}, representing the required output current from the FC's boost converter (I_{fc_out}). Then use the SC and buck/boost converter output to meet the demand by continually updating the value of I_{sc_out}, using:

$$Isc_{out} = I_{load} - Ifc_{ref} \tag{2}$$

where Isc_{out} is the output current from the buck/boost converter, Ifc_{ref} is the user defined reference value for boost converter output current and I_{load} is current going in and out to the load. Using Eq. (2), the SC output current is determined as simply the difference between the load current and the FC reference current values. Eq. (2) can be substituted into Eq. (1) as:

$$Ifc_{out} + I_{load} - Ifc_{ref} = I_{load}$$

$$Ifc_{out} = Ifc_{ref} \tag{3}$$

where Ifc_{out} is the output current of the FC boost converter. As a result, the SC and buck/boost converter output will be required to constantly adjust to match the load demands ensuring the FC and boost converter output is controlled at the reference value. It is worth noting that the FC output is passive in this system and is managed by direct control of the SC output current. This hybrid control system not only keeps the FC output controlled but also takes advantage of the high power density of the SC within the system. By maintaining a controlled and stabilised FC output, dynamic stresses applied to the FC can be significantly reduced, which not only allows improved FC efficiency optimisation, but also potentially extends the FC life by means of a less rigorous duty cycle.

Results

A series of experiments have been carried out to evaluate the developed laboratory hybrid drivetrain and the proposed control strategy. Two sets of experiments were performed: steady state and dynamic tests. The steady state tests were carried out to test the proposed current control strategy for the three operational modes described in Section Hybrid drivetrain operation mode. The dynamic tests investigated the dynamic response of the FC/SC hybrid system and controller against two dynamic drive cycles. Each of these tests are designed to test the operation of the system following the tests proposed in Section Introduction. The quasi-steady state tests are intended to test the fundamental operation of the control strategy and to validate that the performance of each mode of operation can be achieved using the proposed control strategy. From this point, the quasi-steady state tests will be referred to as steady state tests. The Dynamic tests are intended to validate that the system can operate in and change between each of the modes of operation, first for a simple drive cycle and second for a transient drive cycle which is more representative of a city driving bus in real-world operation and hence allows for testing of the system performance under more realistic conditions. The experimental data was collected from multiple sources and logged using the same LabVIEW program developed to control the hybrid system. Measurements of the current and voltage were taken using current and voltage transducers and communicated to the control program through a CAN bus for the input and output data of the bi-directional converter and through an analog input signal through an Advantech USB 4704 data processor for the remainder of the current and voltage data. The logging time interval was set at 50 ms. The motor speed was logged through the motor's encoder signal via an ArduinoMega 2560, again with a 50 ms logging time interval. The raw data was then imported into Matlab where processing and analysis of the data was carried out using a specifically written code.

Steady state test

The steady state tests investigate the performance of the system for each of the modes of operation outlined in Section Hybrid drivetrain operation mode. The FC's boost converter output current (power) was controlled by the proposed current control strategy. The motor current (power) was controlled by varying the throttle and brake commands. The SC was charged/discharged to ensure the load current (power) was always the algebraic sum of the current (power) from the FC and the SC. Each operational mode was tested in the FC/SC hybrid drivetrain with constant values for the currents I_{fc_out}, I_{sc_out} and I_{load}. In each case, the SC is either charging or discharging so it was necessary to prevent any sudden changes to the FC output that would occur as a result of the SC overcharging or undercharging. As such for modes 1 and 2 the tests were run with a SC SoC range of between 20% and 90%. For the test of mode 3 operational conditions, a slightly different approach was taken, the negative value of I_{load} was provided by using regenerative braking to reduce the speed of the flywheel from an initial speed of 4000 rpm, until the braking could no longer provide the desired regenerative current. A number of tests were carried out for each of the modes of operation, with a sample of modes 1, 2 and 3 shown in Figs. 6–8 respectively.

Fig. 6 shows the power balancing in the FC/SC hybrid system and the SoC of the SC in operational mode 1, where the SC discharges to supplement the FC in providing the load power
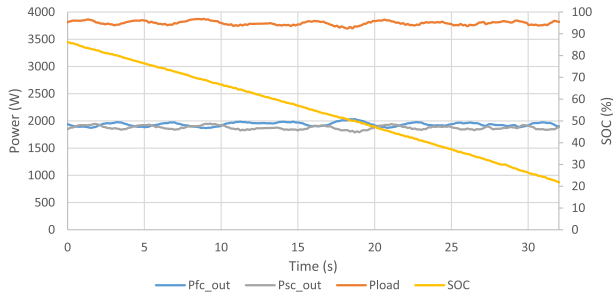
Fig. 6 − Power balancing and SoC for mode 1 operation where the SC discharges and supplements the FC to meet the motor demand.
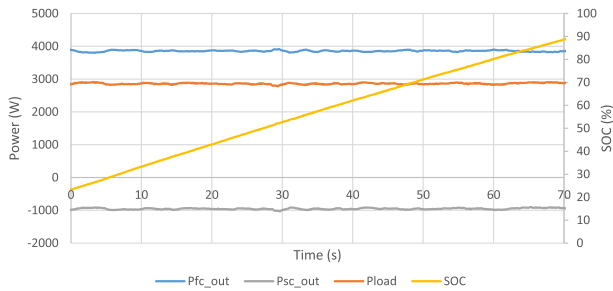

Fig. 7 − Power balancing and SoC for mode 2 operation. The FC supplies the motor load demand where the excess power charges the SC.
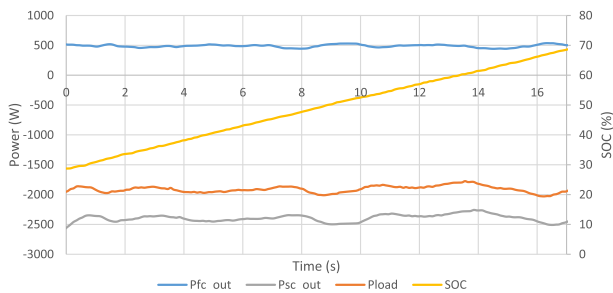

Fig. 8 − Power balancing and SoC for mode 3 operation. The SC is charged from the FC and the regenerative power from the motor.

requirements. In this experiment, the FC and boost converter output current (I_{fc_out}) was selected to be a 40 A constant output by the operator and the load current (I_{load}) demand was maintained at 80 A. As a result, the SC and buck/boost converter (I_{sc_out}) was required to provide a 40 A discharge current to supplement the FC output. The voltage of the common busbar was maintained at 48 V throughout the experiment. As Fig. 6 shows, the FC and boost converter output provided a near constant 1.9 kW power output and was supplemented by the SC and buck boost converter which provided a 1.9 kW output power. The motor power demand (3.8 kW) was met by the algebraic sum of the FC and SC outputs. The SC SoC decreases from an initial value of 85%−22% in 32 s in order to

keep the FC and boost converter output controlled at the user defined value. It should be noted that the slight variations in the plot of P_{FC_out} seen in the figures are caused by noise from the current transducer in the laboratory rig.

Fig. 7 shows the power balancing in the FC/SC hybrid system and the SoC of the SC in operational mode 2, where the SC is charged by the surplus current from the FC. In this experiment, the FC and boost converter output current (I_{fc_out}) was selected to be 80 A and the load current demand (I_{load}) was set at 60 A current. The SC was expected to be charged with the extra 20 A current from the FC. Fig. 7 shows the FC and boost converter provided the expected 3.8 kW (80 A * 48 V) output. The load power 2.9 kW (60 A * 48 V) was met by the FC and the extra power of 1.0 kW (20 A * 48 V) was used to charge the SC. The SC SoC was increased from an initial 22% to a final 89% SoC in 70 s.

Fig. 8 shows the power balancing in the FC/SC hybrid system and the SoC of the SC in operational mode 3, where the SC is charged from both the FC and the output from regenerative braking. In this experiment, the FC and boost converter current (I_{fc_out}) was selected to provide a 10 A current output. A 40 A current will be provided by the motor through regenerative braking by decelerating the flywheel. As Fig. 8 shows, the FC and boost converter provided 0.5 kW (10 A * 48 V) power output. The motor worked as a generator driven by the flywheel and provided 1.9 kW (40 A * 48 V) of regenerative power. From Fig. 8 it can be seen that there are some fluctuations in the motor power, this was a result of the manual control of the motor brake command. It is interesting to note that the SC charge rate mirrors these fluctuations, whilst the FC output remains stable. The SC and buck/boost converter charge rate equalled the sum of both power sources, at 2.4 kW, with the SC SoC increasing from 28% to 68% in 17 s.

In addition to validating the operation of the system with the proposed control strategy, the efficiency of each of the components in the propulsion system was calculated for different loads, as shown in Tables 3−5. It is necessary to understand the efficiency of each of the system components if the overall system efficiency is to be understood and eventually optimised. The FC efficiency was determined from the energy content of the hydrogen consumed (LHV) and the FC electrical energy output. The boost converter efficiency was determined from the electrical energy output of the FC and the electrical energy output of the boost converter. The SC converter efficiency was determined from the input energy of the SC converter and the change in energy of the SC. The motor efficiency was calculated from the electrical energy input to the motor controller and the mechanical energy output. The efficiency of the boost converter and SC converter is fairly stable over the range of loads, with average efficiencies in the range of 90% and 93% respectively. The FC efficiency varies considerably with load, reaching a peak value of 0.534 for I_{fc_in} = 116 A. At higher loads the efficiency slowly drops, however for low loads the efficiency drops away significantly for values of I_{fc_in} < 52 A. When the FC and boost converter efficiencies are combined the peak efficiency is again found to occur at I_{fc_out} = 60 A, with a value of 48.3%. This indicates that the optimal load for minimising hydrogen consumption is for I_{fc_out} = 60 A. This value is stable for high loads, however drops off for low loads as a result of the drop in FC efficiency and

Table 3 – Efficiency of the fuel cell and boost converter for varying load.

Fuel cell loading											
Load (%)	3.1	6.5	11.9	18.5	24.6	31.2	37.9	44.2	51.4	57.8	63.4
I_{fc_out} (A)	5	10	20	30	40	50	60	70	80	90	100
I_{fc_in} (A)	8.1	17.2	32.4	52.3	72.3	93.2	116.0	139.7	170.1	199.1	220.6
Fuel cell											
Efficiency (%)	24.8	36.9	45.4	50.0	51.9	53.0	53.4	53.4	53.3	52.7	52.4
Boost converter											
Efficiency (%)	86.9	87.9	91.4	91.9	92.3	90.8	90.4	89.7	88.4	88.4	86.7
FC and boost converter combined											
Efficiency (%)	21.6	32.4	41.5	46.0	47.9	48.1	48.3	47.9	47.1	46.6	45.4

Table 4 – Efficiency of the supercapacitor converter for varying load.

SC charge								
I_{SC_out} (A)	10	20	30	40	50	60	80	100
Efficiency (%)	90.5	92.2	93.4	92.2	95.3	90.9	89.8	88.4
SC discharge								
I_{SC_out} (A)	−10	−20	−30	−40	−50	−60	−70	−75
Efficiency (%)	98.7	99.4	98.8	96.7	95.0	93.5	97.3	96.5

Table 5 – Efficiency of the motor for varying load, where a negative value indicates regenerative current and a positive value is for a load current.

Traction motor								
I_{load} (A)	−40	−30	−20	−10	20	40	60	80
Efficiency (%)	77.0	75.1	71.5	60.9	72.3	75.2	80.0	82.4

indicates that low load operation of the fuel cell should be avoided where possible. The motor efficiency increases with load up to a value of 82.4% for I_{load} = 80 A. Although this indicates that it would be beneficial to operate the motor at higher loads, it is evident that the motor is required to provide the propulsion for the bus and so the load can't directly be chosen. In terms of the overall system efficiency, the FC efficiency appears to be the most important of the controllable values since it varies significantly with load.

From the results presented it is clear that it is possible to operate the developed FC/SC hybrid propulsion system in each of the desired modes of operation, whilst maintaining a stable output from the FC.

Dynamic tests

The previous results have shown that the FC/SC hybrid system can operate as desired under steady state conditions. To further validate the applicability of the test bench two dynamic tests were carried out to test the performance of the system under transient conditions whilst maintaining a steady FC output. The first was a simple acceleration, constant speed and deceleration test. The second was a more complex dynamic load with multiple changes in speed and was intended to represent the more complex driving cycles that would be expected in real driving conditions. The purpose of these tests is to validate and analyse the performance of the

proposed control strategy under the transient conditions expected for a city driving bus.

Simple dynamic test

A basic driving cycle was initiated, with initial conditions of the flywheel at standstill, the SC charged to 70% SoC. Using a value of I_{fc_ref} of 15 A, the flywheel was then accelerated to 3000 rpm and then maintained a constant speed before being decelerated to standstill through regenerative braking. It should be noted that the braking applied to the flywheel was through regenerative braking only. At speeds below 200 rpm the motor controller decreases the braking applied by the motor and hence the rate of deceleration begins to tail off below this speed. In a real bus system, a mechanical brake would be required to act in parallel with the regenerative brake to provide the braking requirements of the bus. The implementation of the basic driving cycle on the hybrid system not only allowed evaluation of the controller against a dynamic load but also tested the system performance in all three operation modes and the interchange between these modes. The load applied by the load motor is a constant torque value, set at 5% of the maximum motor torque.

Fig. 9 shows the flywheel speed, representing the speed of the bus, and the throttle and brake commands of the drive motor which represent the driver commands. As the figure shows, the motor started to accelerate at 115 s following the throttle command. The throttle command was reduced at 147 s in order to reduce the acceleration and avoid an overshoot of the flywheel speed. The flywheel speed was then maintained at a constant speed of 3000 rpm until 212 s at which point the throttle command was set to zero and the
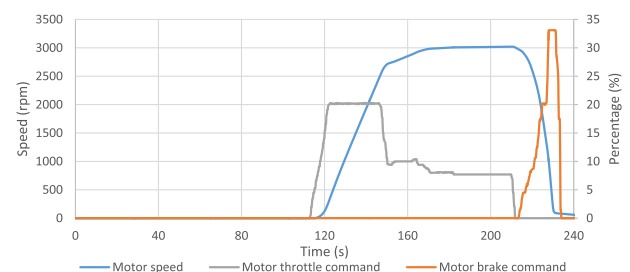

Fig. 9 – Motor speed, throttle command and brake command of the dynamic test. The system is initially at rest followed by an increase in the throttle to accelerate the motor. The motor speed is then kept constant before the brake command increases to decelerate the motor.

brake command increased. The flywheel momentum was used to drive the motor and provide regenerative power depending on the brake command until the flywheel speed reduced to below 200 rpm. It was seen that the driving cycle used for the dynamic test can represent the bus in a number of different conditions which are standstill (0 s–113 s), acceleration (113 s–147 s), constant speed operation (147 s–212 s) and deceleration with regenerative braking (212 s–230 s) which includes all three operation modes.

Fig. 10 shows the power balancing and SoC of the FC/SC hybrid system when the driving cycle described in Fig. 9 was applied. In this test a FC and boost converter output current (I_{fc_out}) of 15 A was selected, with each of the different modes of operation clearly labelled on Fig. 10.

In the first period (0 s–125 s), the bus was at standstill and the FC and boost converter output current (I_{fc_out}) was used to charge the SC, increasing the SoC from 0% to 70%. This is a special case of operation mode 2, where $I_{load} = 0$ A. Initially the FC output current is ramped up to 15 A to protect the FC against a sudden change in FC output. At a time of 113 s the motor begins to accelerate the flywheel, however initially the power requirements of the motor are less than the power provided by the FC and hence the system still operates in mode 2, although the charge rate of the SC begins to decrease, with a maximum SoC of 75%.

In the second period, the flywheel continues to accelerate (125 s–170 s), during this period the motor current requirement (I_{load}) exceeds the FC output current (I_{fc_out}) and hence the SC discharges to supplement the FC output and meet the motor load requirement. This represents operation mode 1. Initially the flywheel accelerates quickly leading to a high motor power requirement. As was previously mentioned the throttle command was reduced at 147 s to avoid a speed overshoot. This is no different to what a driver would be doing in reality. At this point there is a sudden reduction in the motor power requirement, however this still exceeds the FC power output and hence the system still operates in mode 1. During this period, the SC discharges from an SoC of 75%–45%.

In the third period of constant speed operation (170 s–212 s), the motor power demand is significantly reduced as the only load acting on the system is provided by the load motor. In this case the FC power output is greater than the motor power demand, with the excess power being used to charge the SC. During this time the system is operating

in mode 2, with low charge rate of the SC. During this period the SC SoC increased from 45% to 50%.

In the fourth period of regenerative braking (212 s–230 s), the brake command is increased for the drive motor, such that it operates as a generator and engages regenerative mode. As a result, the flywheel decelerates from 3000 rpm down to 200 rpm. During this period the SC is charged by both the FC and the regenerative power from the motor, representing operation mode 3. It can be seen that the regenerative power peaks at 2.4 kW at 224 s, this is supplemented by the FC output of 0.7 kW. This resulted in a rapid increase in the SC SoC from 50% at 210 s to 83% at 230 s.

In the final period between 230 s and 240 s, the flywheel speed is low and the regenerative braking is disengaged. At this point the FC continues to charge the SC until the FC is turned off at 238 s.

This dynamic test proved that the controller is capable of switching between different operational modes while keeping the FC and boost converter output power near constant at the user defined value. Throughout this driving cycle the FC output current was maintained at 15 A and demonstrates that the developed control strategy was capable of operating under the applied conditions whilst meeting the load power demands.

Complex dynamic test

The dynamic test demonstrated the controller is capable of operating with the basic driving cycle. This section aims to evaluate the system performance for a more complex transient driving cycle as frequent start, stop and speed changes are expected to occur during typical city bus driving cycles. The speed profile used for this driving cycle test, SoC change and power balancing have been plotted in Figs. 10 and 11.

Fig. 11 shows the speed profile in the driving cycle test with more speed transients, in terms of both magnitude and rate of change, than the preceding tests. This is used to represent a city bus driving cycle where constant changes in vehicle speed are expected. The SoC generally decreases when the speed increases and vice versa during periods of deceleration. Fig. 12 shows the power balancing of the hybrid system. The value of I_{fc_ref} was set at 20 A which provides a power output of 960 W. The load power and SC power varied more significantly in the driving cycle test when compared with the previous tests. The

Fig. 11 – Motor speed and SC SoC change for the complex driving cycle test. Initially the SC charges with the motor at rest. The motor then goes through numerous accelerations and decelerations which result in a decrease and increase in the SC SoC respectively.
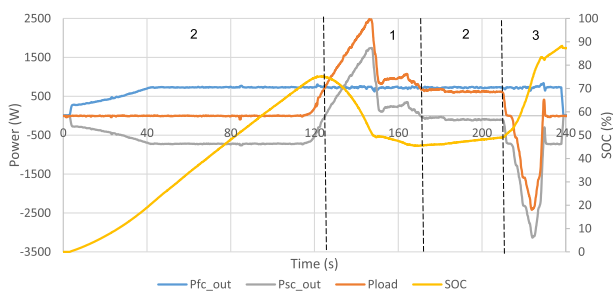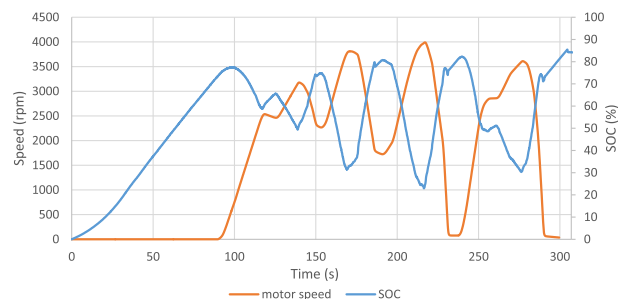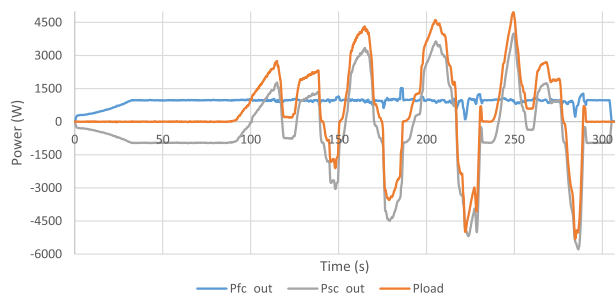

Fig. 10 – Power balancing and SC SoC for the simple dynamic test, where the numbers 1, 2 and 3 refer to the operation mode of the FC/SC hybrid system.

Fig. 12 — Power balancing on the common busbar of the FC/SC hybrid propulsion system for the complex driving cycle test. The FC output is kept relatively stable, with the SC meeting the transient motor power demand.

level of I_{fc_out} was maintained constant throughout most of the test and the large transient load demands were met. However, it can be seen that the FC and boost converter output power varied in three instances with large transient load changes. The fluctuations observed were one overshoot at 186 and two drops at 222 s and 289 s and highlight some of the limitations of the system.

The overshoot at 186 s showed the FC and boost converter output power had increased from the reference value of 960 W–1500 W for approximately 2 s before it recovered to the reference value. It was determined this overshoot was caused by a combination of the large transient change in load demand and a half second gap in the update of the SC current reference in the LABVIEW software. This could be resolved through improving the data processing in the control program.

The two transient drops at 222 s and 289 s were found to be caused by a different reason. To investigate the transient drops, the SC input current (I_{sc_in}) and the bus bar voltage have been plotted in Fig. 13. It is evident that there were voltage spikes to 60 V at both 222 s and 289 s. The SC input current was held at a constant 150 A during these periods. The SC input current cannot exceed 150 A for this test bench as this is the operating current limit of the buck/boost converter. Both of these phenomena result from the large regenerative power outputs and relatively low values of the SC SoC that are present in these time periods. The regenerative power output in each of these cases peaks at over 4.5 kW. When this is combined with the reference FC power output the current required
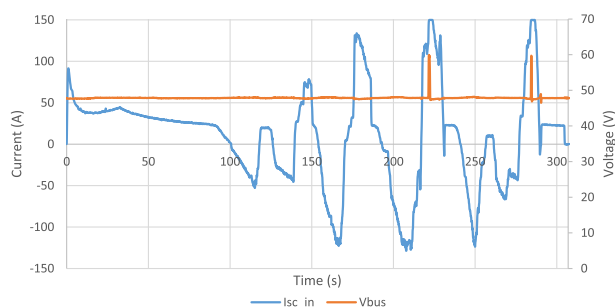

Fig. 13 — SC input current and system bus bar voltage for the driving cycle test. The busbar voltage is maintained at 48 V for the majority of the test. Spikes in the voltage occur when the 150 A current limit for the bi-directional converter is reached.

to transfer this power to the SC (I_{SC_in}) requires a current in excess of 150 A. Since the SC converter is limited to 150 A, the amount of power transferred to the SC is less than that being provided by the sum of the FC and regenerative braking from the motor. As a result, the voltage on the busbar is increased as the motor controller attempts to deliver the power to the SC. However, the SC converter prevents this. This results in a drop in the FC output as there is an excess of power on the busbar and it limits the power the FC can deliver to the busbar at this increased voltage. The drop in FC power output lowers the value of I_{SC_in} required to transfer the available power down to 150 A and hence the busbar voltage recovers to 48 V as there is no longer an excess of power on the busbar. During this period the SC is still being charged, however at a lower rate than is optimum for the system in this configuration. As the SC charges, it's voltage and SoC increase, this increase in voltage reduces the value of I_{SC_in} required to transfer the available power hence the FC was able to return to the reference value of I_{fc_out}. It should be noted that although the system is not operating as desired during these periods, the system is able to continue to operating and recovers to the desired operating state. This situation can be avoided by using a buck/boost converter with higher current carrying capabilities or by maintaining a higher SoC of the SC. It must be noted that the charging voltage of the SC from the buck/boost converter, if low will require a larger charging current. If the SoC is higher, then the charging voltage of the SC from the buck/boost converter will be higher requiring a lower current for the same power transfer. However, this does demonstrate one of the performance limitations of the current system.

The complex dynamic test showed that the proposed system was capable of operating in a transient driving cycle. Since it is expected that a city driving bus will have a very transient load profile it is critical that any proposed control strategy is capable of responding to these transient changes whilst operating as desired. The FC and boost converter current output (I_{fc_out}) was maintained at a constant value and the SC is capable of responding to the transient motor power demands required by the duty cycle in most situations. It was shown that even though there were operating limitations in the system, the FC/SC hybrid control system was capable of recovering to the desired state.

Conclusion

This paper presents the development of a Fuel Cell/Supercapacitor hybrid propulsion system for city bus applications. A laboratory test bench was constructed to represent a scaled power system of a FC/SC hybrid powertrain. A novel control strategy focused on maintaining a constant FC output was developed and proposed specifically for FC hybrid bus applications.

The aim was to develop a system and control algorithm capable of meeting the transient power demands expected for a city driving bus whilst maintaining a constant and user defined FC output. Unlike using the unidirectional boost converter to control the FC output power, the proposed control strategy takes a different approach by using the buck/boost converter for the SC as the decision variable to control

the FC output power in the hybrid system. The proposed control strategy was evaluated with a series of steady state and dynamic tests. It was demonstrated that the control strategy is capable of keeping the FC output constant at a user defined value whilst also maintaining a stable busbar voltage, although the results highlighted some performance limitations of the system. The SC was used to meet the transient load demands of the system and for recovering regenerative power. The proposed control strategy takes advantage of the high energy density of the FC and high power density of the SC. It has been shown that a simple approach can be taken to provide for transient power demands whilst maintaining a stable and constant FC output, avoiding the need for complicated control algorithms and variations in the FC output seen in much of the literature. This has the potential to reduce the stress on the FC but also holds the potential of always operating the FC at its peak efficiency.

A stabilised FC output can significantly mitigate the stress applied on the FC and hereby extend the FC stack life. Further work is required particularly in relation to the protection of the FC from sudden changes in demand that could result from overcharge or undercharge of the SC and in the design procedure for component sizing, particularly in the case of the SC. The research completed is to be used as the basis from which a FC/SC hybrid propulsion system can be designed to meet the performance requirements of a city driving bus whilst optimising the system in terms of capital costs and overall system efficiency. It is acknowledged that the specifics of the hybrid propulsion system will be heavily dependent on the power cycle expected for the bus, with analysis of the particular power cycle necessary to define the component sizing and operational control parameters.

Acknowledgement

REFERENCES

[1] IEA. CO_2 emissions from fuel combustion highlights. Iea; 2015. https://doi.org/10.1787/co2-table-2011-1-en. S/V:10.
[2] IEA. Energy and CO_2 emissions in the OECD. 2017.
[3] TfL. Improving the health of Londoners — transport action plan. Gt London Auth; 2014.
[4] Barbir F. PEM fuel cells theory and practice. Elsevier Academic Press; 2005.
[5] Hayre RO, Cha SW, Colella W, FBP. Fuel cell fundamentals. 2016. Hoboken, New Jersey.
[6] Moreno NG, Molina MC, Gervasio D, JFPR. Approaches to polymer electrolyte membrane fuel cells (PENFCs) and their cost. Renew Sustain Energy Rev 2015;52:897—906.
[7] Eberle U, Muller B, RVH. Fuel cell electric vehicles and hydrogen infrastructure: status 2012. Energy Environ Sci 2012;2012(5):8780.
[8] Nilsson M, Hillman K, Rickne A, TM. Paving the road to sustainable transport: governance and innovation in low carbon vehicles. Routledge — Business and Economics; 2012.

[9] Li Y, Li J, Qin Z, ZW. Development of fuel cell hybrid electric city bus. In: Transp Electrif Asia-Pacific IEEE Conf Expo; 2014.
[10] Hoffmann P, BD. Tomorrow's energy: hydrogen, fuel cells and the prospects for a cleaner planet. MIT Press; 2012.
[11] Wu B, P MA, Yufit V, De Benedetti L, Veismann S, Wirsching C, et al. Design and testing of a 9.5kW proton exchange membrane fuel cell supercapacitor passive hybrid system. Int J Hydrogen Energy 2014;39:7885—96. https://doi.org/10.1016/j.ijhydene.2014.03.083.
[12] Li Q, Yang H, Han Y, Li M, WC. A state machine strategy based on droop control for an energy management system of PEMFC battery supercapacitor hybrid tramway. Int J Hydrogen Energy 2016;41:16148.
[13] Wu W, Partridge J, Bucknall R. Development and modelling of a lab scaled PEM fuel cell drive system for city driving application, 2016. Coimbra, Port: UPEC; Sept. 6-9th 2016.
[14] Melo P, Ribau J, CS. Urban bus fleet conversion to hybrid fuel cell optimal powertrains. Procedia Soc Behav Sci 2014;692.
[15] Bubna P, Advani SG, AKP. Integration of batteries with ultracapacitors for a fuel cell hybrid transit bus. J Power Sources 2012;199:360.
[16] Xie C, Xu X, Bujilo P, Shen D, Zhao H, SQ. Fuel cell and lithium iron phosphate battery hybrid powertrain with an ultracapacitor bank using direct parallel structure. J Power Sources 2015;279:487.
[17] Li Tianyu, Liu Huiying, Dingxuan C, Zhaoa D, W L. Design and analysis of a fuel cell supercapacitor hybrid construction vehicle. Int J Hydrogen Energy 2016;41:12307—19. https://doi.org/10.1016/j.ijhydene.2016.05.040.
[18] Andaloro L, Napoli G, Sergi F, Dispenza G, Antonucci V. Design of a hybrid electric fuel cell power train for an urban bus. Int J Hydrogen Energy 2013;38:7725—32. https://doi.org/10.1016/j.ijhydene.2012.08.116.
[19] Sergi F, Andaloro L, Napoli G, Randazzo N, Antonucci V. Development and realization of a hydrogen range extender hybrid city bus. J Power Sources 2014;250:286—95. https://doi.org/10.1016/j.jpowsour.2013.11.006.
[20] Napoli G, Micari S, Dispenza G, Di Novo S, Antonucci V, Andaloro L. Development of a fuel cell hybrid electric powertrain: a real case study on a minibus application. Int J Hydrogen Energy 2017;42:28034—47. https://doi.org/10.1016/j.ijhydene.2017.07.239.
[21] Andaloro L, Arista A, Agnello G, Napoli G, Sergi F, Antonucci V. Study and design of a hybrid electric vehicle (Lithium Batteries-PEM FC). Int J Hydrogen Energy 2017;42:3166—84. https://doi.org/10.1016/j.ijhydene.2016.12.082.
[22] Latha K, Umamaheswari B, Chaitanya K, Rajalakshmi N. A novel reconfigurable hybrid system for fuel cell system. Int J Hydrogen Energy 2015;40:14963—77. https://doi.org/10.1016/j.ijhydene.2015.08.031.
[23] Talpone J, Puleston PF, More JJ, Grino R, Cendoya MG. Experimental platform for development and evaluation of hybrid generation systems based on fuel cells. Int J Hydrogen Energy 2012;7:2—9. https://doi.org/10.1016/j.ijhydene.2012.01.161.
[24] Benyahia N, Denoun H, Zaouia M, Rekioua T, Benamrouche N. Power system simulation of fuel cell and supercapacitor based electric vehicle using an interleaving technique. Int J Hydrogen Energy 2015;40:15806—14. https://doi.org/10.1016/j.ijhydene.2015.03.081.
[25] Torreglosa JP, Jurado F, Garcia P, Fernandez LM. PEM fuel cell modeling using system identification methods for urban transportation applications. Int J Hydrogen Energy 2011;6. https://doi.org/10.1016/j.ijhydene.2011.03.133.
[26] Bougrine MD, Benalia A. Nonlinear adaptive sliding mode control of a powertrain supplying Fuel Cell Hybrid Vehicle. In: Proceedings of the 3rd International Conference on

Systems and Control, Algiers, Algeria, 29th–31st October, 2013; 2013.

[27] Fares D, Chedid R, Karaki S, Jabr R. Optimal power allocation for a FCHV based on linear programming and PID controller. Int J Hydrogen Energy 2014;39:21724–38. https://doi.org/10.1016/j.ijhydene.2014.09.020.

[28] Allaoua B, Asnoune K, Mebarki B. Energy management of PEM fuel cell/supercapacitor hybrid power sources for an electric vehicle. Int J Hydrogen Energy 2017;42:21158–66. https://doi.org/10.1016/j.ijhydene.2017.06.209.

[29] Feroldi D, Carignano M. Sizing for fuel cell/supercapacitor hybrid vehicles based on stochastic driving cycles. Appl Energy 2016;183:645–58. https://doi.org/10.1016/j.apenergy.2016.09.008.

[30] Ettihir K, Cano MH, Boulon L, Agbossou K. Design of an adaptive EMS for fuel cell vehicles. Int J Hydrogen Energy 2016;42:1481–9. https://doi.org/10.1016/j.ijhydene.2016.07.211.

[31] Fathabadi H. Novel fuel cell/battery/supercapacitor hybrid power source for fuel cell hybrid electric vehicles. Energy 2018;143:467–77. https://doi.org/10.1016/j.energy.2017.10.107.

[32] Behdani A, Naseh MR. Power management and nonlinear control of a fuel cell e supercapacitor hybrid automotive vehicle with working condition algorithm. Int J Hydrogen Energy 2017;42:24347–57. https://doi.org/10.1016/j.ijhydene.2017.07.197.

[33] Bougrine M, Benalia A, Delaleau E. Minimum time current controller design for two- interleaved bidirectional converter: application to hybrid fuel cell/supercapacitor vehicles. Int J Hydrogen Energy 2017:1–13. https://doi.org/10.1016/j.ijhydene.2017.07.188.

[34] Luo X, Wang J, Dooner M, Clarke J. Overview of current development in electrical energy storage technologies and the application potential in power system operation. Appl Energy 2015;137:511–36. https://doi.org/10.1016/j.apenergy.2014.09.081.